Development of an Automated Microinjection System for Batch Manipulation of Carbon Nanotube Sensors

Selina C. Qu, Carmen K. M. Fung, Rosa H. M. Chan and Wen J. Li

Centre for Micro and Nano Systems
The Chinese University of Hong Kong
Hong Kong SAR

wen@acae.cuhk.edu.hk

***Abstract* - A novel automated Carbon Nanotube (CNT) microinjection system for batch fabrication of a bulk multi-walled carbon nanotubes (MWNT) based MEMS sensor is presented. The basic process includes AC electrophoretic manipulation of MWNT bundles on a silicon substrate. By utilizing this technology, CNTs were successfully and repeatably manipulated between micro-fabricated electrodes. Besides, the devices were demonstrated to potentially serve as novel thermal sensors with low power consumption (~ μW) and fast frequency response (~ 100kHz). Based on these experimental evidences, a feasible batch manufacturable method for functional CNT sensors by using the automated injection system is developed which will dramatically reduce production costs and production time of nano sensing devices and potentially enable fully automated assembly of CNT based devices.**

Index Terms* - *AC electrophoretic manipulation, carbon nanotube, CNT sensors, nano manufacturing, nano batch fabrication.

I. Introduction

Carbon nanotubes (CNTs), has been widely studied for its electrical, mechanical, and chemical properties since its discovery. In order to build a CNT based device, fast and batch techniques to manipulate the CNT has to be developed. Typical manipulation technique is by atomic force microscopy [1]. However, this pick-and-place technique is time consuming, which is unrealistic for batch fabrication. Past demonstrations by K. Yamamoto et al. showed that carbon nanotube can be manipulated by AC and DC electric field [2][3]. Besides, a recent report from L. A. Nagahara et al. demonstrated the individual single-walled carbon nanotube (SWNT) manipulation using nano-electrodes by AC bias voltage [4]. By using similar technique (i.e., AC electrophoresis), we have successfully manipulated bundled carbon nanotubes to form resistive elements between Au microelectrodes for sensing and electronic circuits efficiently. However, in our prior work, we found that the yield of the batch assembly of the CNT devices cannot be 100% as the volume of each drop of the CNTs/ethanol solution during the CNT manipulation can be varied. Therefore, in order to improve the yield, a precise and automated CNT injection system is developed. This paper reports the technique to form bundled MWNT resistive element between Au electrodes. Our experimental results agree well with computer simulations that modeled the connections of nanotubes between various electrode configurations in different dielectrophoretic (DEP) force fields. Accordingly, Ac electrophoresis makes the batch fabrication of nano devices using nanotubes as components feasible. In addition, we have proven that carbon nanotube devices built by this method are capable of performing very low power thermal sensing (i.e., ~1000 times lower than conventional MEMS polysilicon based thermal sensors) and can be fabricated in a fast and efficient manner [5]. The detailed process to manipulate nanotubes using AC electrophoresis and the experimental results from using the carbon nanotube bundles as thermal sensing elements will be presented. In addition, the preliminary CNT microinjection system will be presented. The results indicate that the carbon nanotube is promising to be used as high performance and low power consumption devices for future electronic and sensing applications.

II. AC Electrophoretic Manipulation of CNT

In our carbon nanotubes manipulation experiments, the carbon nanotubes were dispersed inside a liquid medium (e.g., ethanol), therefore other forces (e.g., viscous force), other than the dielectrophoretic forces are also imparted on the carbon nanotubes during the manipulation process. In order to understand the physical phenomenon during the dielectrophoretic manipulation, we conducted the following simulations on the effect of different microelectrode geometries on carbon nanotube alignments. The results were also validated experimentally.

A. Theoretical Background and Modeling

AC electrophoresis (or dielectrophoresis) is a phenomenon where neutral particles undergoing mechanical motion inside a non-uniform AC electric field. Detailed descriptions on AC electrophoresis can be found in [6].

With negligible gravitational force, the three main force components are the DEP force, the viscous force and the electro thermal force. For other small particles with their volumes compatible to MWNT, the thermal effects can dominate, but the high polarizability of MWNT makes the DEP force large enough to produce the deterministic movements.

Dielectrophoresis refers to the force exerted on a polarized particle in a non-uniform electric field [6][7]. It can be written as

$$\boldsymbol{F}_{\boldsymbol{DEP}}(t) = (\boldsymbol{m}(t)\cdot\nabla)\boldsymbol{E}(t) \qquad (1)$$

where E is the electric field, m is the induced dipole moment of MWNT. Assumed that the MWNT is a long prolate spheroid with the longest axis aligned with the electric field, the induced dipole moment is

$$\boldsymbol{m}(t) = 4\pi\varepsilon_m ab^2 K\boldsymbol{E}(t) \qquad (2)$$

where ε_m, K, a and b are the absolute permittivity of the medium, the complex polarization factor, the half length of MWNT and the radius of MWNT, respectively. Since the electric field components are in phase, the time averaged DEP force deduced from the above equations is

$$< \boldsymbol{F}_{\boldsymbol{DEP}}(t) >= 2\pi ab^2\varepsilon_m \,\mathrm{Re}(K)\nabla \mid \boldsymbol{E}_{rms} \mid^2 \qquad (3)$$

where $\nabla \mid \mathrm{E}_{rms} \mid^2$ is the gradient of the square of the root-mean-square of the electric field.

Frequency of the applied voltage also affects the magnitude of DEP force as the complex permittivity spectra of MWNT and ethanol are the functions of the frequency [8][9][10]. Because of the high conductivity of the assumed purified MWNT (≈2.22 x 10^4S/m) [8] and the small depolarization factor resulted from its long dipole ($L_{\parallel} \approx 8.3434$ x 10^{-5}), the real part of the complex polarization factor is positive as shown in Fig. 1. Although the actual complex polarization factor varies, which is because the absolute permittivity and the orientation of each MWNT varies [8], Re(K) remains positive. When substituting different permittivity values at 1MHz, the DEP force is maximum when the longest axis is parallel to the electric field (Re(K)≈3995.2). By substituting $L_{\parallel}$ with $L_{\perp} \approx 0.5$ in (3), the minimum DEP force can be calculated when it is perpendicular to the field (Re(K)≈0.6667). The corresponding positive dielectrophoretic force draws the MWNT to the electric field maxima.

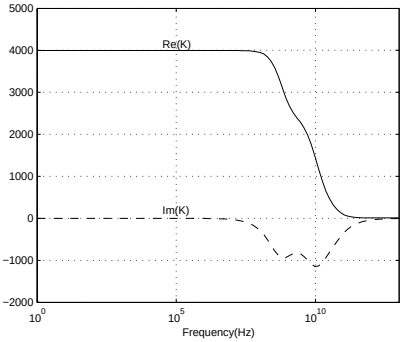

Fig. 1. Complex polarization factor K when the longest axis of the MWNT is parallel to the electric field applied.

An array of microelectrodes is fabricated and the CNT connections across the microelectrodes by the dielectrophoresis are shown in Fig. 2. Details of the experimental procedures for the dielectrophoretic manipulation of MWNT will be presented in the next section. On the other hand, in order to visualize the electric field distribution generated by pairs of microelectrodes, simulations have been conducted and described in the following part.

The approximate order of the potential was investigated by using Green's theorem [11], and the square root-mean-square magnitude of the field was calculated by using MatLab. Since the magnitude of the electric field decreases with height from the electrodes, the positive DEP draws the MWNT downwards to the edges of the electrodes. The force fields in Fig. 3 are estimated by (3), assuming that the longest axes of MWNT is parallel to the instantaneous electric field.

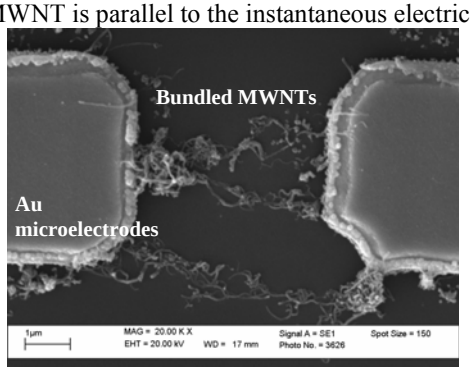

Fig. 2. Scanning electron microscopic (SEM) image showing the MWNT connections between Au microelectrodes.

Downward forces are shown by the contours in Fig. 3 between the electrodes and close to the electrode surfaces. The DEP forces are significantly large to draw the MWNT downwards and to overcome the upward movement from the electro thermal effect [12].

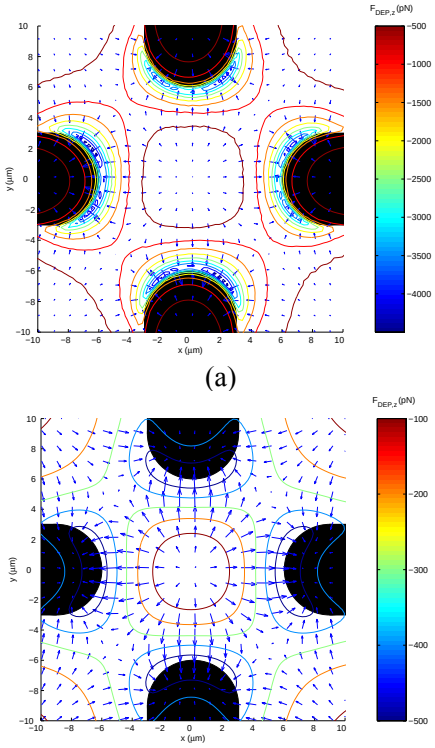

Fig. 3. Average DEP force between the electrodes which were applied by the 16V peak-to-peak AC voltage at 1MHz. The arrows are the force vectors on x-y plane (a) at 1 μm and (b) 3 μm, respectively, above electrodes in Fig. 2. The contours represent the order of downward forces.

B. *Experimental Details and Results*

Based on the physical phenomenon of AC electrophoresis, we have successfully manipulated the bundled CNTs on fabricated microelectrodes. The experimental process flow for the CNTs manipulation can be divided into three parts: fabrication of microelectrodes, sample preparation and experimental testing (see Fig. 4).

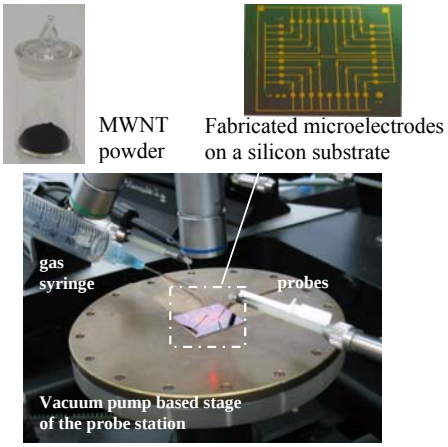

Fig. 4. Experimental setup for CNT manipulation by using AC electrophoresis.

The Au microelectrodes were fabricated on glass or Si/SiO_2 substrates by a standard microfabrication technique, which was described previously in [13]. Prior to the MWNT manipulation, bundled MWNTs were prepared by a sonication treatment. The bundled MWNTs used in the experiments were ordered commercially from [14] which were prepared by chemical vapour deposition. The axial dimension and the diameter of the MWNTs was 1 – 10 μm and 10 – 30 nm, respectively. In order to form stable colloidal suspension of MWNTs and minimize the degree of aggregation, 50 mg of the sample was ultrasonically dispersed in 500 mL ethanol solution and the resulting solution was diluted to 0.01 mg/mL for later usage.

During the CNTs manipulation, a substrate with fabricated Au microelectrodes was placed on the vacuum pump based stage of a micromanipulator station, which allowed the probing of microelectrodes by microprobes. Au microelectrodes were then excited by an AC voltage source with typically of 16 V peak-to-peak with frequency of 1 MHz. Approximately 10μL of the MWNTs/ethanol solution was transferred to the substrate by a 6 mL gas syringe. The ethanol was evaporated away leaving the MWNTs to reside between the gaps of the microelectrodes. We have observed from the experimental results that bundled MWNTs was attracted towards the Au microelectrodes under non-uniform electric field and connected across the microelectrodes. A representative scanning electron microscopic (SEM) image showing the bridging of MWNTs across the Au microelectrodes is shown in Fig. 2.

The formation of MWNTs linkages can be further confirmed by testing the connectivity between the pair of microelectrodes. For instance, room temperature resistances between the microelectrodes were measured and the two probe room temperature resistances of the samples typically range from several kΩ to several hundred kΩ, which suggested the connection had been formed between the two microelectrodes.

As mentioned in the pervious section, AC electrophoretic manipulation is different from those traditional pick-and-place manipulations (e.g., AFM manipulation) which can only assemble CNT devices one at a time. Instead, AC electrophoretic manipulation is a parallel assembly process where batch assembly of CNT devices is theoretically possible when the electrical potential is applied to an array of microelectrodes which are connected electrically together. To prove the validity of batch assembling by AC electrophoresis, we have implemented the experimental procedures mentioned and extended to an array of Au microelectrodes which are electrically connected together on a substrate (see Fig. 5). By using the same experimental parameters presented before, we have successfully manipulated the CNT bundles on most of the Au microelectrodes by AC electrophoresis in a single-run fashion. The connections of bundled CNTs for different pairs of microelectrodes on a substrate after addition of one drop of MWNTs/ethanol solution (~ 10μL) were shown in Fig. 6. In order to confirm the linkage of bundled CNTs across two microelectrodes, the room temperature resistance corresponding to each pair of microelectrodes was measured. The CNT connection process was deemed successful between 2 microelectrodes when the room temperature resistance measured became several kΩ to several hundred kΩ. Several chips were then checked using a scanning electron microscope (SEM) to validate the CNT connections between the electrodes.

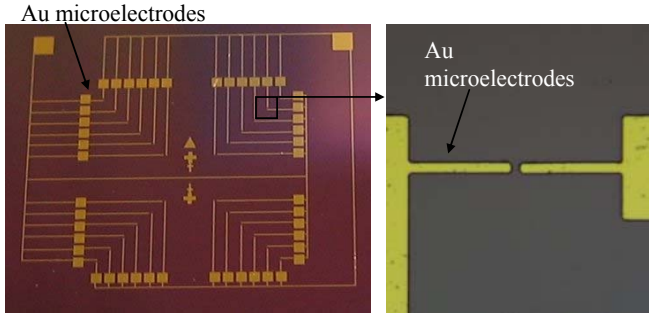

Fig. 5. (a) Photograph of the fabricated array of Au microelectrodes on a substrate. (b) Optical image showing a pair of Au microelectrodes before CNT manipulation.

To validate the consistency of the batch assembly of CNT devices, repeated experiments for AC electrophoretic batch manipulation of CNTs between the arrays of Au microelectrodes were performed and plots of statistical data for different experiments were generated (see Fig. 7), which

shows the maximum, minimum, average and standard deviation (S. D.) among the measured resistances on each sample. From the experimental results, we have observed that the range of the room temperature resistances is from several kΩ to several hundred kΩ as stated earlier. Besides, we have experimentally found that the success rate for different sensor chips are consistent with overall success rate, which is equal or greater than 70%. The success rate is defined as the ratio of the number of successful CNTs-connected microelectrodes to the total number of microelectrodes on a substrate. Since the volume of each drop of the CNTs/ethanol solution in the experiment is not consistent, the yield of the batch assembly of the bundled CNTs cannot be 100% based on our current rudimentary technique. However, the batch AC electrophoretic manipulation of bundled CNTs is efficient and reliable based on our experimental validation, and the yield can be further improved by using a more precise injection system, which will be described in the later section.

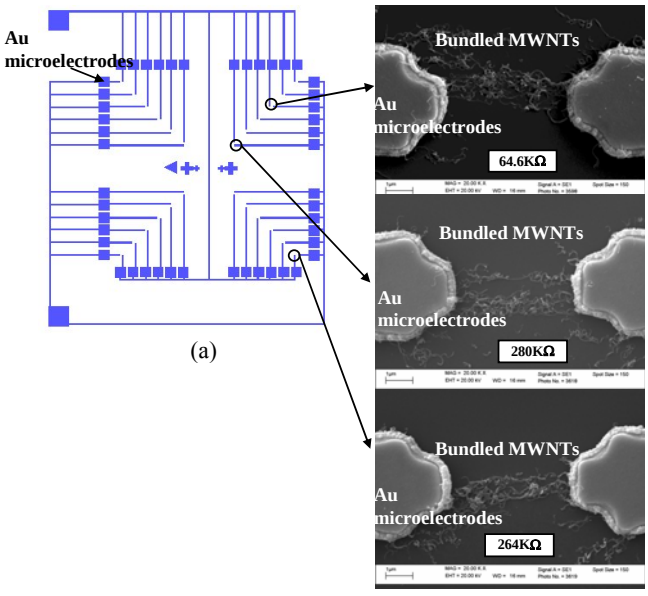

Fig. 6. (a) Drawing of the design for the chip with arrays of Au microelectodes. (b) Scanning electron microscopic (SEM) images showing the formations of MWNTs between different pairs of Au microelectrodes.

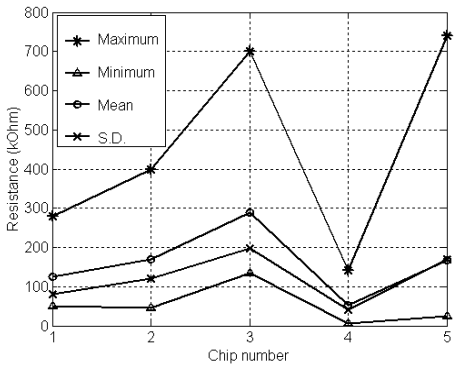

Fig. 7. Plots of statistical data of measured resistances between the Au microelectrodes on different samples.

III. CNT AS SENSING ELEMENTS

With the ability to batch manipulate the bundled CNTs to form resistive elements on patterned substrates, we have investigated the possibility to utilize the bundled CNTs as sensing elements for thermal sensing. The bundled MWNTs as sensing elements for micro thermal sensors can be driven by a simple constant current circuit. An experiment for investigating the temperature dependence of the bulk MWNT sensor was performed. The fabricated sensor chip was packaged on a PCB for data acquisition and was put inside an oven. Then, the resistance change of the MWNT sensors was measured as the temperature inside oven was varied. The temperature-resistance relationship for the MWNT sensors was measured and a representative data set is shown in Fig. 8 for several cycles of measurements. From the experimental results, the bundled MWNT resistance dropped with temperature. Other than the first measurement cycle, the resistance at room temperature converged and the slopes were consistent for each measurement. The negative TCR of the MWNTs had been reported previously in [15], although the measurements were based on individual MWNTs. As reported in [15], the variations in resistivities and temperature resistance dependency of CNT are due to the interplay of changes in carrier concentration and mobilities in the metallic tubes. Therefore, the linear relationship of the resistance and temperature of our bundled CNT sensor can be predicted and the behavior of resistance decreasing with increasing temperature is possibly dependent on the intrinsic thermal properties of the MWNTs. The temperature-resistance dependency of bundled MWNT implies its thermal sensing capability. Based on experimental results, the range of the temperature coefficient of resistance (TCR) for the MWNT sensors were found to be from -0.04 to -0.07 $\%/^{O}C$.

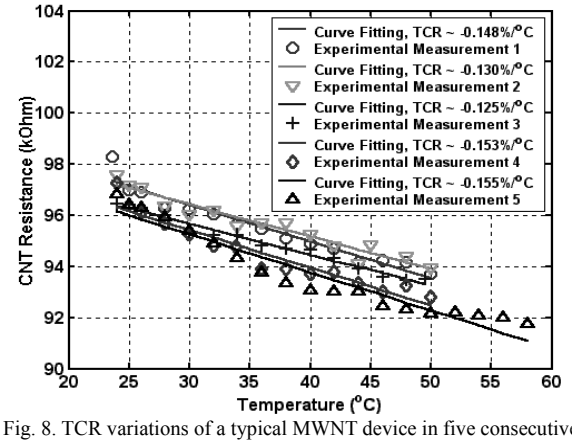

Fig. 8. TCR variations of a typical MWNT device in five consecutive measurements. The experimental data are linearized for the approximation of TCRs.

The I-V Characteristic of the MWNT sensors was also investigated. From the results of experiments conducted on the MWNT sensors, the current required to induce self heating of the MWNT devices was in μA range at several volts, which

suggests that the power consumption of these devices is in the μW range (see Fig. 9).

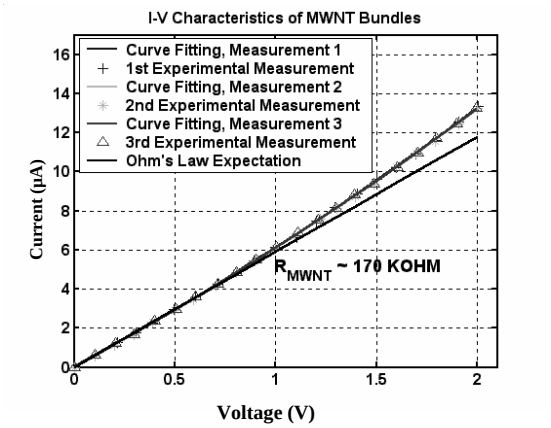

Fig. 9. I-V characteristics of the MWNT bundles. Three repeated measurements were performed to validate the repeatability. The straight line is the theoretical expectation using Ohm's Law and the room temperature resistance of bundled MWNTs in our testing sample was about 170kΩ.

Investigation on the frequency response of the MWNT sensor was also carried out. To test the frequency response of the embedded bundled MWNT sensor, input square wave of 3V peak-to-peak at 19 kHz was fed into the negative input terminal of the circuit and the output response was observed on an oscilloscope (see Fig. 10). From our experimental measurements, bundled MWNT sensors exhibited very fast frequency response (about 148 kHz). As a comparison, typical frequency response of MEMS polysilicon sensors in constant current mode configuration without frequency compensation is around several hundred Hz to several kHz [16][17].

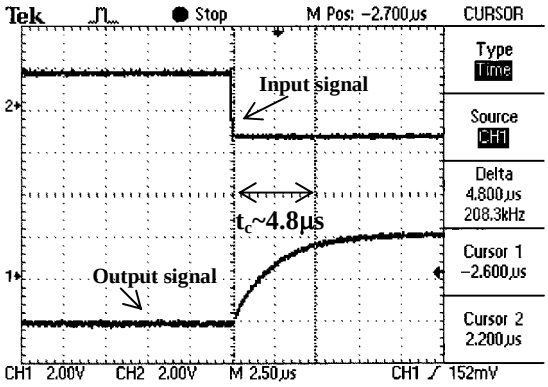

Fig. 10. Frequency response of MWNT bundles in constant current mode.

IV. Automated CNT Microinjection System

Based on the results of CNT formation by using AC electrophoresis process and the thermal sensing capability of the bundled CNT sensor, we are now developing a computer-controlled CNT microinjection system for performing the dielectrophoresis CNT manipulation automatically. The preliminary prototype of the CNT microinjection system is illustrated in Fig. 11 and the experimental setup of the system can be shown in Fig. 12. It mainly consists of three parts: motorized manipulators, a set of video microscope system, and a computer. The whole system is installed on a vibration isolation table.

A chip with sensors-microelectrodes and the ethanol/CNT solution are placed on a x-y motorized plate. A nano probe fabricated in [18] is fixed on another manipulator and moves in z direction, which is used to transfer the solution on the microelectrodes. In order to obtain an image data of the chip, a video microscope is used to observe the position of the gaps of the microelectrodes in the chip.

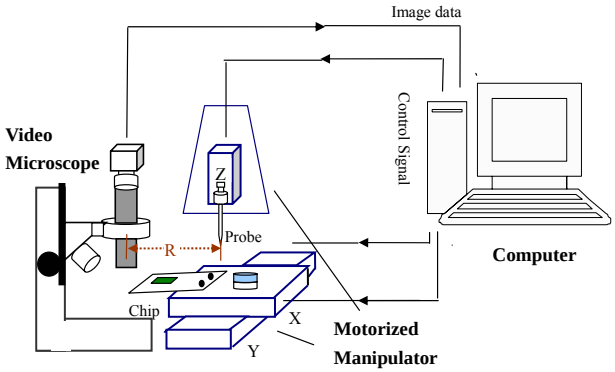

Fig. 11. The architecture of the CNT microinjection system.

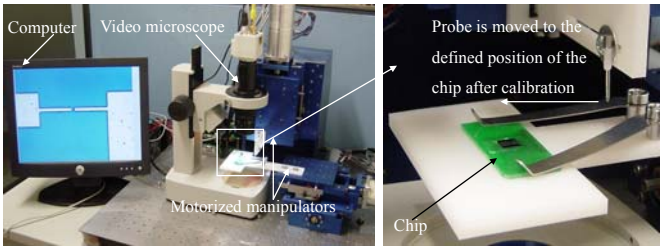

Fig. 12. The experimental setup of the CNT microinjection system.

A. *Calibration of the system*

Before the injection process, calibration is done to obtain an exact relative position between the view field of the microscope and the accurate X-Y-Z framework, which is denoted by *R* shown in Fig. 11. It is noted that R are three dimensional, i.e., *R*=(*Rx*, *Ry*, *Rr*), representing the distances in X and Y directions, and the rotation angle. The illustration for obtaining R is shown in Fig. 13. To do this, a sample chip for calibration is firstly put on the X-Y stage, and the position of the chip is set as the origin. Afterwards, the nano probe with Z-stage is moved downwards to transfer a droplet on the chip. The X-Y stages are moved and the probe drops another droplet on the chip. By repeating this process several times, a matrix of droplets is obtained ($\sum_1$ in Fig. 13). The X-Y stages are then commanded to move to the view filed of the microscope, i.e. $\sum_1$ is moved to $\sum_2$, which is observed in the screen as $\sum_3'$. The angle *Rr* is the angle between the digital video and the microscope. The matrix of the droplets is observed in the screen and noted as $\sum_3$. During the

movement of X-Y stage described above, the moving distance is recorded and noted as *Rx* and *Ry* for X and Y directions respectively. Thus, the exact relative position R is obtained.

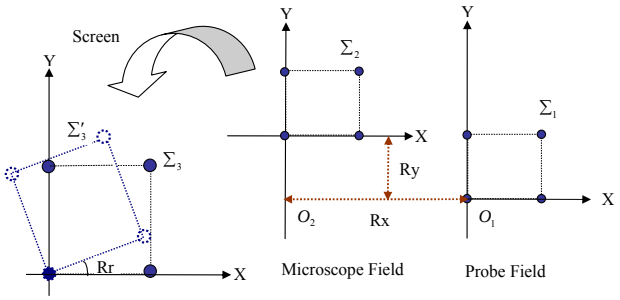

Fig. 13. Illustration of the calibration of the system.

B. *Injection process*

After obtaining the relative position *R* of the sample chip and the probe, the chip with array of electrodes is put on the X-Y stage and its position is adjusted in the field view of the microscope so that the relative position of the chip and the probe is same as the position *R* obtained in the calibration process. As some parameters such as the position of each microelectrodes and the distance between each microelectrodes *D* (see Fig. 14) are defined, the injection process is done by the computer program automatically. In that work, the X-Y stages with the chip are moved with the relative position R such that one of the microelectrodes of the chip is exactly under the probe, the probe on the Z-stage is then commanded to move downwards to drop the solution on the microelectrodes. The X-Y stages are repeatedly moved according the parameters set in the pervious processes and the probe transfers the solution to the rest of the microelectrodes.

The principle of the injection process of the probe can also be shown in Fig. 14. From Fig. 14, the probe is dipped into the solution, it can pick up a small amount of the solution because of the capillarity action. Afterwards, the probe is commanded to move by the manipulator to make the probe close and touch the chip at the prescribed position, to drop the solution in the certain position of the chip.

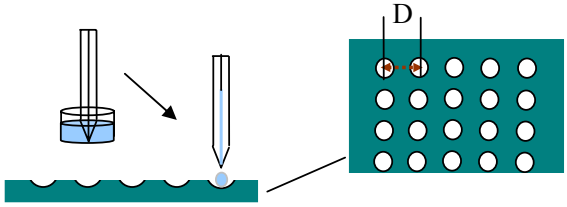

Fig. 14. Illustration of the injection process.

ACKNOWLEDGMENT

Funding for this project was provided by The Chinese University of Hong Kong (CUHK). The authors would like to sincerely thank Dr. W.Y. Cheung of the Department of Electronic Engineering of CUHK and Mr. Victor T. S. Wong of the Department of Mechanical and Aerospace Engineering of University of California for their help and discussion on this project.

REFERENCES

[1] T. Shiokawa, K. Tsukagoshi, K. Ishibashi, Y. Aoyagi, "Nanostructure construction in single-walled carbon nanotubes by AFM manipulation", *Microprocesses and Nanotechnology Conference 2001*, pp. 164 – 165, 2001.

[2] K. Yamamoto, S. Akita, Y. Nakayama, "Orientation of carbon nanotubes using electrophoresis", *Japanese J. Appl. Phys.*, vol.35, L917-L918, 1996.

[3] K. Yamamoto, S. Akita, Y. Nakayama, "Orientation and purification of carbon nanotubes using AC electrophoresis", *J. Phys. D: Applied Physics*, vol. 31, L34-L36, 1998.

[4] L.A. Nagahara, I. Amlani, J. Lewenstein and R.K. Tsui, "Directed placement of suspended carbon nanotubes for nanometers-scale assembly", *Appl. Phys. Letters*, vol. 80, No. 20, pp. 3826 – 3828, 2002.

[5] C.K.M. Fung, V.T.S. Wong and W.J. Li "Towards batch fabrication of bundled carbon nanotube thermal sensors", *IEEE NANO 2003*, vol. 2, pp. 866-869, 2003.

[6] H.A. Pohl, "Dielectrophoresis: The behaviour of neutral matter in nonuniform electric fields", *Cambridge University Press*, 1978.

[7] T. B. Jones, "Electromechanics of particles", Cambridge: *Cambridge University Press*, 1995.

[8] C. A. Grimes, E. C. Dickey, C. Mungle, K. G. Ong, and D. Qian, "Effect of purification of the electrical conductivity and complex permittivity of multiwall carbon nanotubes", *J. Appl. Phys*., vol. 90, no. 8, pp. 4134 – 4137, 1995.

[9] P. Petong, R. Pottel, and U. Kaatze, "Water-ethanol mixtures at different compositions and temperatures. A dielectric relaxation study", *J. Phys. Chem. A*, vol. 104, pp. 7420-7428, 2000.

[10] X-B. Wang, Y. Huang, R. Hoizel, J. P. H. Burt, and R. Pethig, "Theoretical and experimental investigations of the interdependence of the dielectric, dielectrophoretic and electrorotational behavior of colloidal particles", *J. Phys. D: Appl. Phys*., vol. 26, pp. 312-322, 1993.

[11] X. Wang, X-B Wang, F. F. Becker, and P. R. C. Gascoyne, "A theoretical method of electrical field analysis for dielectrophoretic electrode arrays using Green's theorem", *J. Phys. D: Appl. Phys*., vol. 29, pp.1649 – 1660, 1996.

[12] T.Heida, W.L.C. Rutten, and E. Marani, "Understanding dielectrophoretic trapping of neuronal cells: modeling electric field, electrode-liquid interface and fluid flow", *J. Phys. D: Appl. Phys*., vol. 35, pp.1592 - 1602, 2002.

[13] V.T.S. Wong, and W.J. Li, "Dependence of AC electrophoresis carbon nanotube manipulation on microelectrode geometry", *Int. J. Nonlinear Sciences and Numerical Simulation.*, vol. 3, nos. 3-4, pp. 769-774, 2002.

[14] Sun Nanotech Co Ltd, Beijing, P.R. China.

[15] T.W. Ebbesen, H.J. Lezec, H. Hiura, J.W. Bennett, H.F. Ghaemi, and T.Thio, "Electrical conductivity of individual carbon nanotubes", *Nature*, vol. 382, pp. 54 – 56, 1996.

[16] C. Liu, J.B. Huang, Z. Zhu, F. Jiang, S. Tung, Y.C. Tai, C.M. Ho, "A micromachined flow shear-stress sensor based on thermal transfer principle", *J.MEMS*, vol. 8, No. 1, pp. 90 – 99, 1999.

[17] J.B. Huang, F.K. Jiang, Y.C. Tai, C.M. Ho, "MEMS-based thermal shear-stress sensor with self-frequency compensation", *Measurement Science and Technology*, vol. 10, No. 8, pp. 687 – 696, 1999.

[18] K.W.C. Lai, W.J. Li, "KL probes for robotic-based cellular nano surgery", *IEEE Nano 2003*, vol. 1, pp. 152 – 155, 2003.